JOM, Vol. 75, No. 8, 2023
https://doi.org/10.1007/s11837-022-05694-2

Fabrication of Mg-Sn-Y/Al6061 Composite Plates by Asymmetrical Rolling with Differential Temperatures and their Microstructures and Mechanical Properties

ZHIHUI CAI,[1,2] ZHENYU WU,[1] LIFENG MA,[1,2,3] YIBO WANG,[1] CHENCHEN ZHI,[1,2] and JUNYI LEI[1]

1.—School of Mechanical Engineering, Taiyuan University of Science and Technology, Taiyuan 030024, Shanxi, People's Republic of China. 2.—Heavy Machinery Engineering Research Center of the Ministry of Education, Taiyuan University of Science and Technology, Taiyuan 030024, Shanxi, People's Republic of China. 3.—e-mail: mlf_zgtyust@163.com

Mg/Al composites were successfully fabricated by the differential temperature + asymmetrical rolling (DTAR) and the isothermal + symmetrical rolling (ISR), respectively. The effects of DTAR and ISR on the tensile properties, bonding strength, interface morphology, and microstructure of composite plates were investigated. The results indicated that grains near the Mg layer of the Mg/Al interface were fine and equiaxed because of the occurrence of dynamic recrystallization on the Mg layer. In contrast, the grains at the center and near the Al side interface were elongated. DTAR enhanced the recrystallization degree of Mg side grains. The tensile properties and bonding strength of the composite plates increased gradually with increase in reduction rate, while the interface morphology was gradually flat with increase in reduction rate. The ultimate tensile strength of DTAR sample reaches 205 MPa, which is 25% higher than that of ISR sample.

INTRODUCTION

Laminated composite plates with a unique performance by combining different material properties have attracted a wide range of attention from researchers.[1,2] Compared with alloys with rare metals, these new-type materials can be widely used in many industries, such as aerospace, electronics, and shipbuilding, because of their excellent properties and low cost.[3,4] Thus, the appropriate selection of matrix and clad materials has a significant meaning in producing composite materials with the desired properties to achieve the goal of energy-saving and emission reduction.

In recent years, Mg alloys have been used in automobiles and high-speed trains because of the distinct merits of low density, high specific strength, and stiffness.[5,6] However, because of the formation of loose and porous oxide film on alloys' surfaces, the active chemical properties of magnesium alloys greatly limit the application of alloys in corrosive environments.[7] There is an urgent need to improve the corrosion resistance of magnesium alloys to broaden their applications. On the contrary, the oxidation on the Al surface can greatly prevent alloys from corroding.[8] Therefore, Mg/Al composite plates are fabricated to take the advantage of component metals.

Mg and Al alloys can be combined by explosive welding,[9] extrusions,[10] and roll bonding.[11] The most widespread production method is roll bonding, which has the advantages of simple equipment and large-scale continuous production.[12,13] However, the Mg/Al composite plates fabricated by the traditional rolling process have some defects, such as easy cracking, severe warping, and poor mechanical properties. The reasons can be concluded to the following: (1) At room temperature, the plastic deformation ability of Mg and its alloys is inferior because of the hexagonal closed pack (HCP) crystal

(Received September 30, 2022; accepted December 29, 2022; published online January 20, 2023)

structure, which will affect the coordinate ability of matrix and clad sheets during the rolling process.[14] On the contrary, prismatic and pyramidal slips of Mg and its alloy can be activated under hot rolling, but the oxide formation in the interface will decrease the bonding strength.[15,16] (2) The incoordinate deformation of matrix and clad sheets will produce residual stress due to the immense strain in the rolling process, making composite plates warp and unable to carry out subsequent processes.

Various new Mg alloys have been developed recently, and Mg-Sn based alloys have attracted great interest among them. The reason is that the addition of the Sn elements not only causes transformation in grain size, secondary phase, and grain orientation distribution,[17] but also reduces the unstable stacking fault energy, resulting in the activation of the slip system.[18] At the same time, the formation of the Mg2Sn phase provides the ability of Mg-Sn based alloys to resist creep at high temperatures.[19] A previous study has reported that Y addition could help Mg alloys maintain excellent ductility and stretch formability at room temperature.[20] Therefore, it has more excellent application prospects for applying Mg-Sn-Y alloys as a substrate material to prepare Mg/Al composite plates.

To overcome the shortcomings of conventional rolling Mg/Al composite plates, a novel rolling method named differential temperature + asymmetrical rolling (DTAR) in this study is proposed to manufacture Mg/Al laminated composites. On the one hand, compared with isothermal + symmetrical rolling (ISR), asymmetrical rolling is beneficial in reducing the critical pressure drop ratio required for dissimilar metal recombination, reducing the rolling force, promoting the shear deformation of the composite plate interface, enhancing the mechanical meshing between dissimilar metals, and improving the quality of interface bonding compared with symmetrical rolling.[21,22] Li et al.[23] studied the effect of asymmetrical rolling on the bonding strength of Al/Cu/Al composite plates and realized stronger interface bonding by providing additional shear deformation by asymmetrical rolling. In recent years, the application of asymmetrical rolling on magnesium alloy has only focused on the effect of single magnesium alloy microstructure[24] and forming properties.[25] Studies on the fabrication of Mg/Al composite plates are still scarce and need further exploration. On the other hand, temperature gradients could decrease the plasticity gap of component metals and improve the deformation uniformity and bond strength of composite plates.[26] Consequently, the DTAR technology is an excellent preparation process for Mg/Al composite plates.

In this study, Mg-Sn-Y alloy and 6061 Al alloy sheets were rolling bonded by the DTAR process at 400°C with different rolling reductions. The composite blanks were also rolled by isothermal + symmetrical rolling (ISR) at identical reductions for contrast to investigate the microstructure evolution, including the interface morphology, grain refinement, and texture, and the differences between DTAR and ISR on the mechanical properties were also discussed.

MATERIALS AND EXPERIMENTAL PROCEDURE

Fabrication of Mg/Al Composite Plates

The results of the previous studies showed that the comprehensive mechanical properties of Mg/Al laminates were better at rolling temperatures of 400°C, rolling speeds of 10 rpm to 20 rpm, and total rolling reductions of 30% to 70%.[27,28] Therefore, the single-pass roll bonding process was carried out at the rolling temperature of 400°C and the rolling speed of 0.1 m/s with the rolling reductions of 40%, 50%, and 60%, respectively.

A Mg-Sn-Y ingot was prepared from high-purity Mg, Sn, and Y, whose chemical compositions are listed in Table I. A resistance furnace (SG5-10) with a power of 5 KW was used for smelting. The magnesium ingot was melted by heating to a temperature between 660°C-720°C, and the protective gas was a mixture of SF_6 and CO_2. After the Mg had been completely melted, the preheated Sn and Y were added into the molten Mg as required. The alloying elements were melted and stirred every 10 min, and the casting was carried out at 650°C. The ingot was firstly solubilized at 345°C/4 h + 500°C/6 h and quenched into the hot water at about 80°C. After heat treatment at 390°C for 90 min before pressing, the extrusion temperature was between 360°C and 370°C, the extrusion speed was 1.05 mm/s, and the extrusion ratio was 16:1. The extruded Mg-Sn-Y alloy and Al6061 alloy were used in this study.

The dimensions of Mg-Sn-Y alloy and 6061 sheets were 100 × 60 × 3 mm and 100 × 60 × 1.5 mm, respectively. The contact surface was cleaned by using a wire brush and acetone to remove the oxides and greases. Riveting with rivets can effectively prevent slippage between dissimilar metals during the rolling process. These assembled sheets were heated in a resistance furnace at 400°C for 15 min under a protective atmosphere. Both ISR and DTAR processes proceeded in a two-roll mill. An upper roller of ∅320 × 350 mm with 150°C and lower roller of ∅224 × 350 mm with 25°C were used in DTAR so that the speed ratio was 1.43. The blanks were rolled by a single pass under the reduction of 40%, 50%, and 60% so that the plates rolled by DTAR were marked as DTAR-40%, DTAR-50%, and DTAR-60%, respectively. Notably, the Mg sheet touched the upper roller with a faster linear speed. Two rollers of ∅320 × 350 mm with 150°C were used in ISR. The blanks were also rolled by single pass under the same reductions, and the plates rolled by ISR were marked as ISR-40%, ISR-50%, and ISR-60%, respectively. A schematic description of the experimental procedure is shown in Fig. 1.

Table I. Specifications of primary sheets

Material	Chemical composition (wt%)	Sheet dimensions
Al6061	97.8 Al, 0.61 Si, 0.23 Fe, 0.26 Cu, 0.002 Mn, 0.98 Mg, 0.001 Zn, 0.01 Ti, and 0.06 Cr	100 × 60 × 1.5 mm
Mg-Sn-Y	99.05 Mg, 0.5 Sn and 0.45 Y	100 × 60 × 3 mm

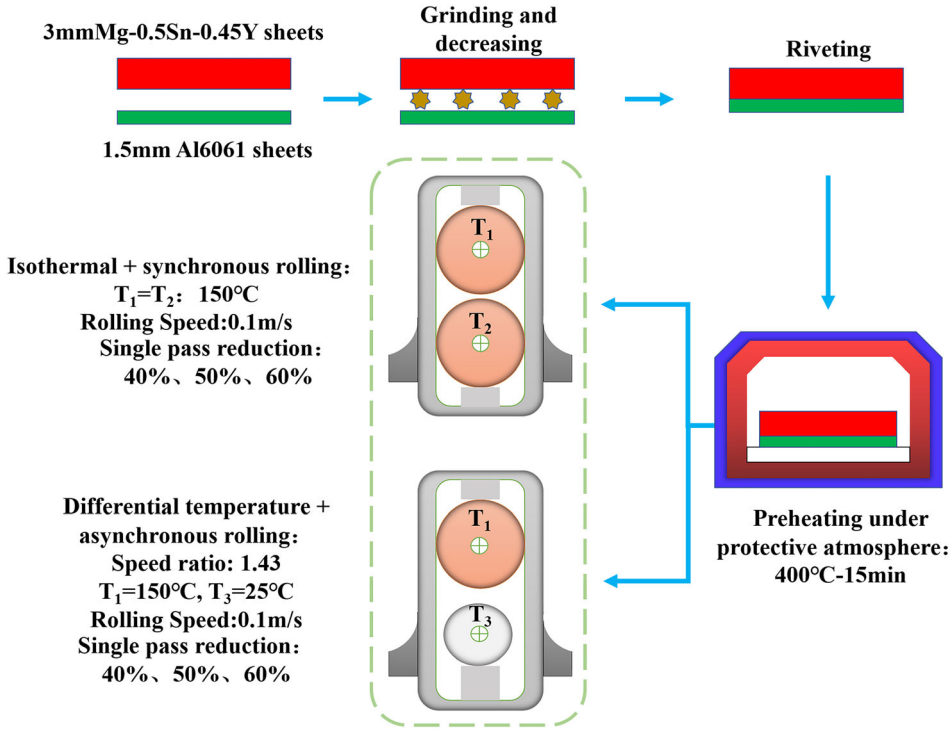

Fig. 1. Experimental procedure schematic of rolling processes.

Microstructure Characterization

The samples were prepared in a direction parallel to the rolling direction for microstructure analysis. Then, they were mechanically polished to a mirror-like surface. With the help of a scanning electron microscope (SEM) and energy-dispersive spectrometer (EDS), composite plate interface morphology and microstructures were characterized. Specimens of electron backscatter diffraction (EBSD) were ground with SiC papers, washed, and electropolished at -25°C. All EBSD data were analyzed using the Channel 5 software.

Mechanical Properties

The uniaxial tensile experiments were carried out at room temperature with a crosshead velocity of 0.75 mm/min, in which an optical extensometer was used. For accuracy, the tensile test was repeated three times. For laminated metal composites, bond strength is an essential criterion for judging whether dissimilar metals achieve good bonding. The bonding strength test was carried out on a universal testing machine at a speed of 0.75 mm/min at room temperature. The dimensions of the specimen for the interface bonding strength test are shown in Fig. 2. The bonding strength can be calculated by Eq. 1.

$$\tau = F/S \quad (1)$$

where the F is the tensile strength load, and the S is the shear area.

RESULTS AND DISCUSSION

Mechanical Properties of Mg/Al Composite Plates

Tensile Properties

Figure 3 illustrates the tensile properties of Mg/Al composite plates with different rolling reductions on ISR and DTAR. Under both processes, the larger the rolling reduction is, the stronger the ultimate tensile strength and yield strength of Mg/Al composite plates, while the elongation showed the opposite trend. In detail, there were also differences

in the comprehensive mechanical properties of the rolled plates under the two processes. The ultimate tensile strength of the composite plates under ISR increased from 173 to 190 MPa, and yield strength increased from 91 to 140 MPa; the elongation decreased from 3.9% to 2.7% when the rolling reductions were 40%-60%. In contrast, the ultimate tensile strength of the composites rolled by DTAR increased from 188 to 205 MPa, and yield strength increased from 100 to 156 MPa, but elongation decreased from 3.1% to 2.1% under the same rolling reductions. It is distinct that the Mg/Al composite plates rolled by DTAR had higher ultimate tensile strength and yield strength but lower elongation.

The higher strength in Mg/Al composite plates rolled by DTAR was mainly attributed to the coupled effects of work hardening and grain refinement strengthening. During the DTAR process, the plate was subject to vertical compressive stress. In addition, owing to the speed difference between the two rollers, the plate was also subject to a pair of shear stresses, which generated shear strain in the direction of the thickness of the plate. Therefore, the deformation caused by single-pass DTAR rolling was more severe than that in the case of ISR. The effect of frictional shear on the component metals was enhanced, contributing more deformation energy into heat energy for the thermal activation of dynamic recrystallization (DRX) and obtaining finer microstructure. According to the Hall-Petch relationship ($\sigma_y = \sigma_0 + kd^{-1/2}$), the degree of grain refinement is inversely proportional to the strength of the plate.[29] Thus, the strength was significantly improved under the DTAR process. However, the higher work-hardening effect was detrimental to the ductility.

Figure 4 shows the tensile fracture morphology of Mg and Al layers along the rolling direction (RD) and the transverse direction (TD) in tensile test samples of ISR-60% and DTAR-60%. There is little difference in the fracture morphology of Al layers of ISR-60% and DTAR-60% samples, which were characterized by uniform dimples, showing a feature of ductile fracture. In contrast, the fracture morphology of Mg layers between samples of ISR-60% and DTAR-60% was different. A small number of dimples accompanied by cleavage planes existed in the ISR-60% sample, indicating that two fracture mechanisms simultaneously occurred. For the Mg layer in DTAR-60% sample, no dimples were observed, accounting for the low ductility of composite plates.

Hardness

The Vickers hardness tests were conducted to investigate the mechanical properties of Mg/Al composite plates under ISR and DTAR. The hardness values were measured from the Mg side to the Al side for the samples with different rolling reductions by ISR and DTAR. As shown in Fig. 5, the hardness of the component metals of rolled composite plates under ISR and DTAR gradually increased with the increase in rolling reduction, and the hardness at the interface showed the same trend. The increase in hardness was attributed to the grain refinement strengthening, which was related to the recovery and recrystallization during the rolling process. Moreover, it is reported that with increasing rolling reduction, the main strengthening mechanism was grain refinement strengthening due to the formation of ultrafine grains.[30]

It is not difficult to find that the overall hardness of composite plates rolled by DTAR was higher than that of the plates rolled by ISR at the same rolling reductions. This is because in the DTAR, the plate deformation zone existed as a cross shear deformation zone, which played a role in refining the microstructure, hindering the dislocation migration during plastic deformation, and increasing the hardness of the component metal. At the same time, Nussbaum et al.[31] pointed out that the shear force introduced during the rolling process resulted in a more pronounced refinement of the second phase of component metal, which had a more significant hindering effect on dislocations, leading to an increase in the overall hardness of plates.

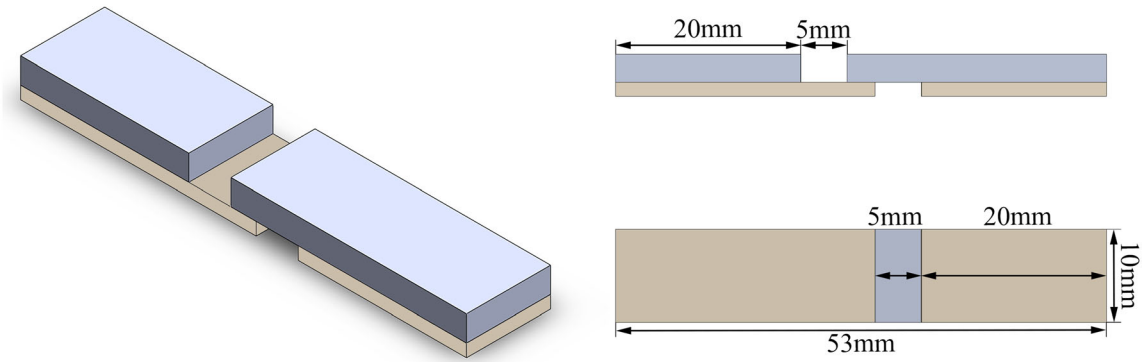

Fig. 2. Schematic drawing of machined specimens for the bonding test.

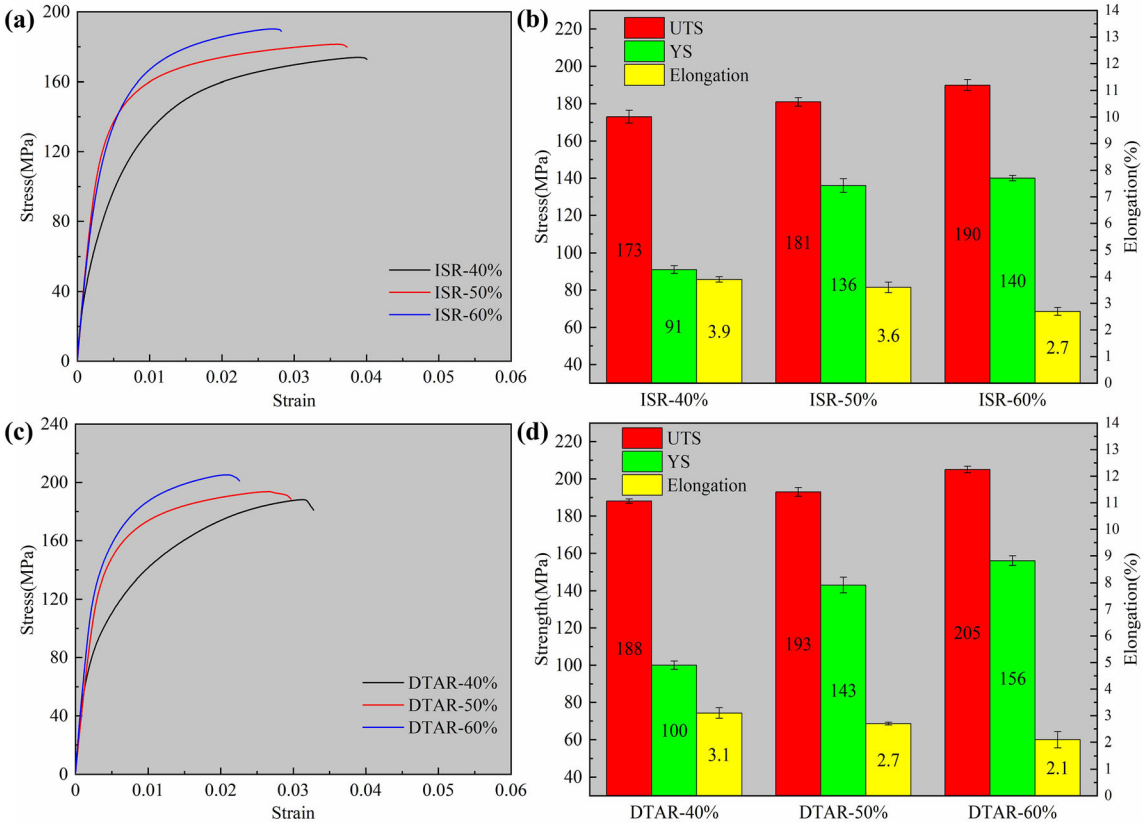

Fig. 3. The stress-strain curves of rolled Mg/Al composite plates by (a, b) ISR and (c, d) DTAR.

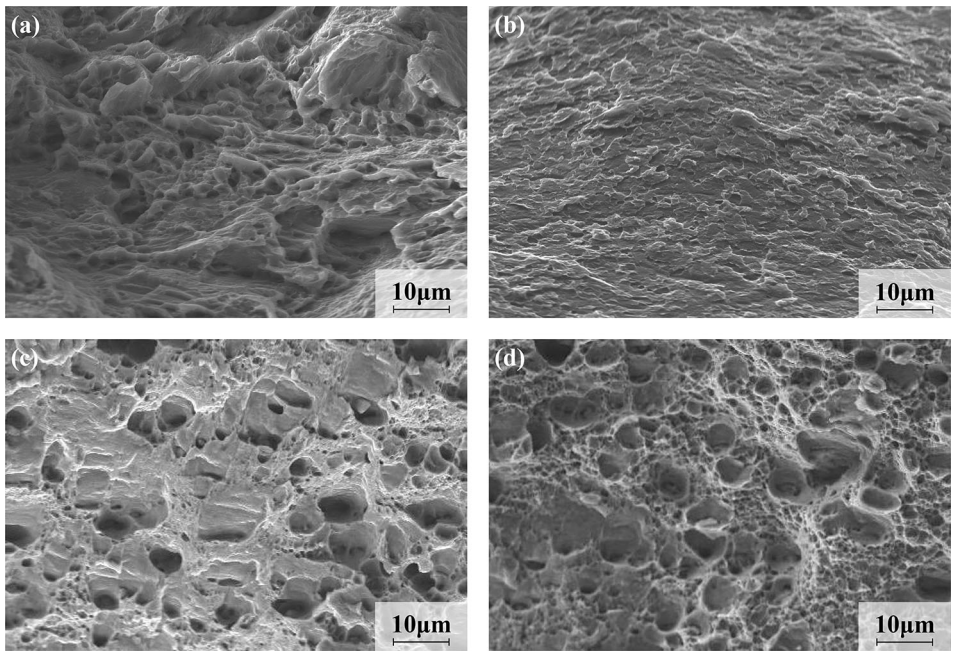

Fig. 4. Fracture images after the tensile tests of Mg/Al composite plates: (a) ISR-60%-Mg; (b) DTAR-60%-Mg; (c) ISR-60%-Al; (d) DTAR-60%-Al.

Bonding Strength

Figure 6 shows the bonding strength of Mg/Al composite plates with different rolling reductions by ISR and DTAR. The bonding strength of plates rolled by both ISR and DTAR increased with the increase in rolling reduction, and notably the

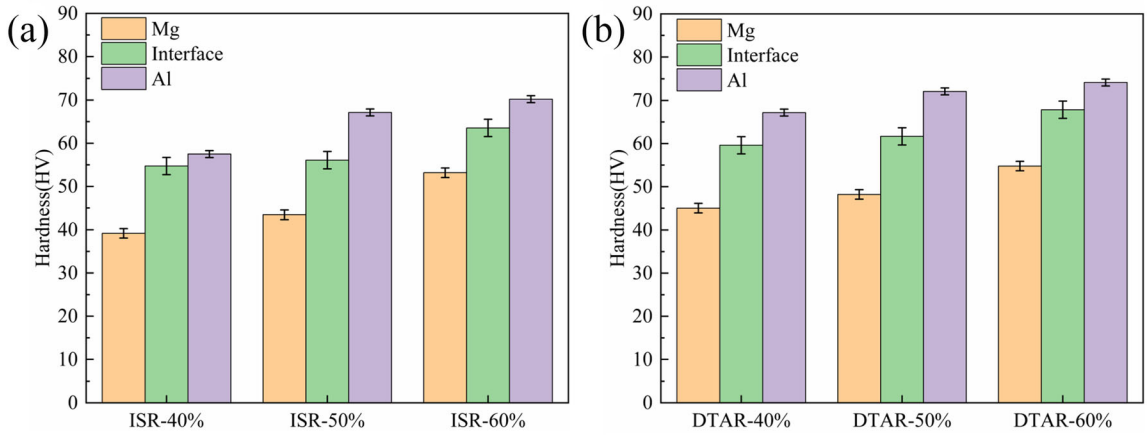

Fig. 5. Hardness variations of rolled Mg/Al composite plates by (a) ISR and (b) DTAR.

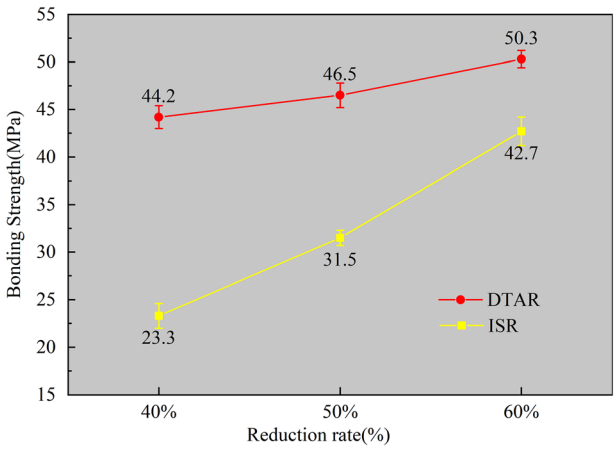

Fig. 6. The bonding strength of rolled Mg/Al composite plates.

bonding strength of the plates rolled by DTAR was higher than that of the plates rolled by ISR under the same reduction.

This phenomenon could be explicated by the following two aspects: (1) It was proposed that shear and normal deformation were the fundamental reasons for the mechanical bonding of composite plate interfaces.[21] Therefore, at the same rolling reductions, the DTAR process promoted the coordinated deformation of component metals and introduced a cross shear deformation zone on the compounded area, which enhanced the frictional shear effect between component metals. Deformation from the normal direction allowed fresh metals near the junction to penetrate each other through surface cracks. In addition, the DTAR process improved the degree of atomic diffusion and promoted the formation of metal bonding between magnesium and aluminum atoms. (2) Compared with ISR, the frictional shear effect during DTAR at the same reduction rates caused significant grain fragmentation and refinement of the matrix metal, which enhanced the degree of DRX within the matrix plates and the bonding between the component metals.

Interface Morphology of Mg/Al Composite Plates

Figure 7a-f shows the SEM image of the Mg/Al interfaces and the corresponding line scan resulting from the different rolling reductions by ISR and DTAR. As shown in Fig. 7a-c, there were no apparent voids or defects in the interfacial regions. However, it is worth noting that the interface morphology of ISR-40% was very rough and uneven (see Fig. 7b and c). The interface morphology became smooth with the increase in rolling reductions. It is well known that the interface was gradually flattened with increasing rolling force, which helped break down the hardening layer of the component metals and promote the exposure of fresh metal. Thus, the bonding mechanism from the mechanical bonding under the low reduction gradually transformed into metallurgical bonding under significant reduction.

Figure 7d-f shows that the samples under DTAR showed relatively straight and tight interfaces, and there were no gaps and holes at the bonding interface. The shear deformation under DTAR produced work hardening promoting the coordinated deformation of component metals. At the same time, it also intensified the friction between contact surfaces, resulting in energy accumulation. The deformation work and the accumulated energy on the interface exposed the fresh metal under the surface, and the composite area expanded. In addition, a temperature gradient reduced the plastic gap between component metals and promoted coordinated deformation during DTAR, so matrix and clad sheets achieved close contact and high bonding strength. From the EDS line scanning across bonding interfaces of the Mg/Al composite plates in Fig. 7a-f, the two lines were X-shaped, and no strictly steep lines appeared, indicating no intermetallic compounds were generated at the

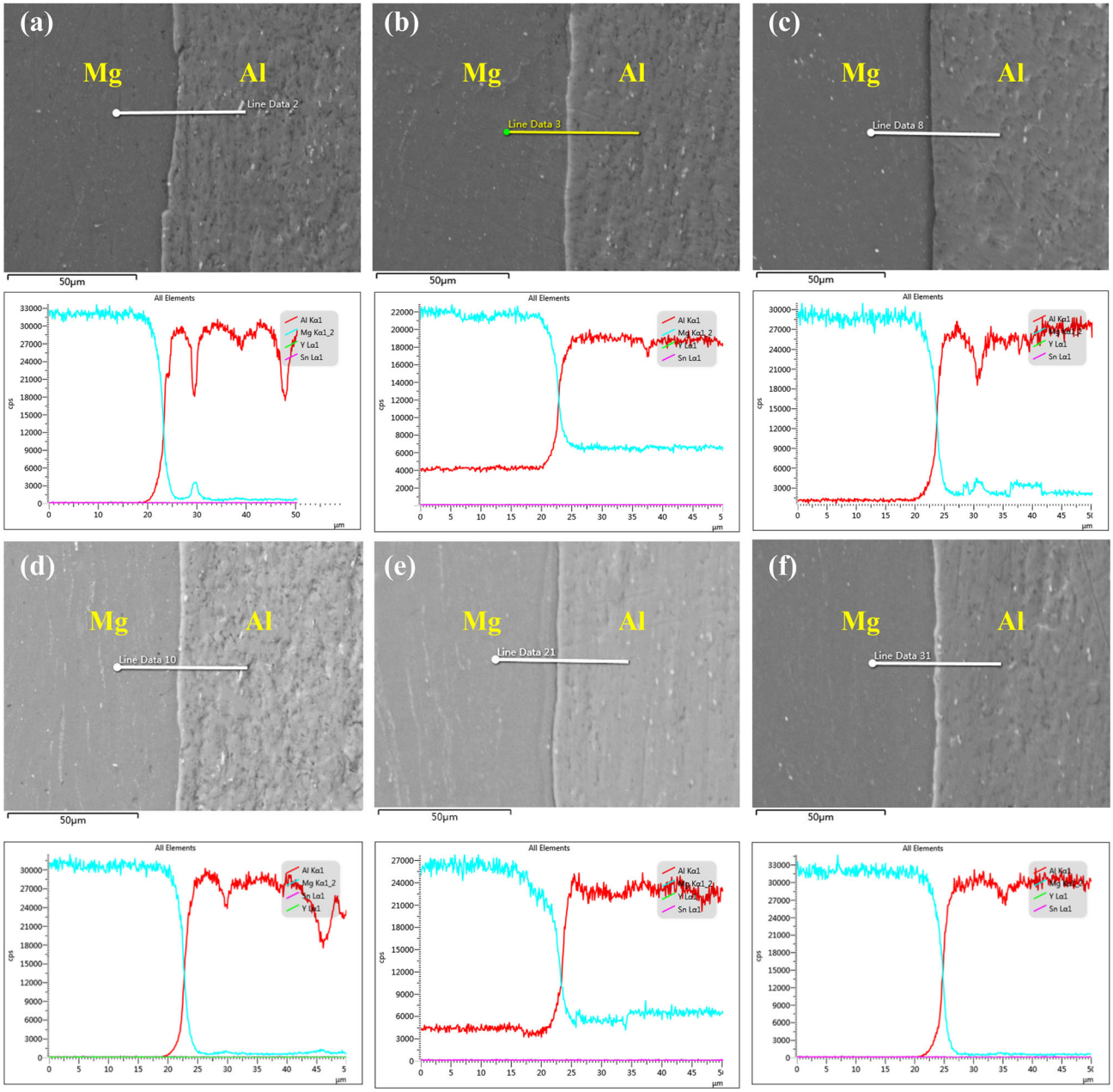

Fig. 7. SEM images of the rolled Mg/Al composite plates: (a) ISR-40%; (b) ISR-50%; (c) ISR-60%; (d) DTAR-40%; (e) DTAR-50%; (f) DTAR-60%.

interfaces. A metallurgical combination at the interface is conducive to improving the bond strength of the composite plate.

Microstructure of Mg/Al Composite Plates

Misorientation Angle

Figures 8 and 9 exhibit the distribution of grain boundary misorientation angle in the matrix and clad layers in as-extruded, ISR-60%, and DTAR-60% plates, respectively. The high-angle grain boundaries (HAGBs, $> 15°$) and low-angle grain boundaries (LAGBs, 2°-15°) are indicated in black and white lines, respectively. It could be noted that the fraction of LAGBs and HAGBs was 0.25 and 0.47 for the Mg layer in ISR-60% sample. However, the percentage of LAGBs decreased to 0.15, HAGBs increased to 0.61, and the average value of misorientation angle of Mg alloy increased to 26.07° in DTAR sample. The enormous deformation provided by DTAR activated many slip systems, which made deformation energy accumulate in Mg layers.[32] Besides, the shear stress in DTAR sample made it possible to convert part of the deformation energy into thermal energy, providing good conditions for the thermal activation of DRX and enhancing the

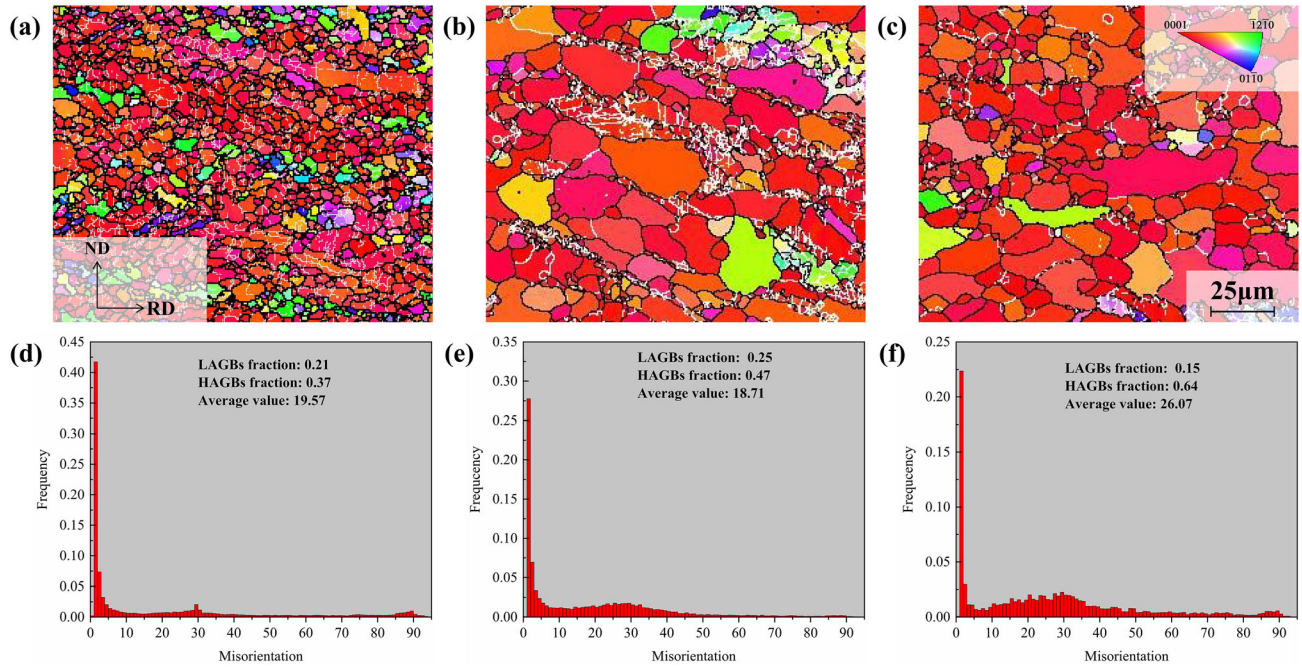

Fig. 8. Distribution of misorientation angle of Mg layer: (a,d) as-extruded; (b,e) ISR-60%; (c,f) DTAR-60%.

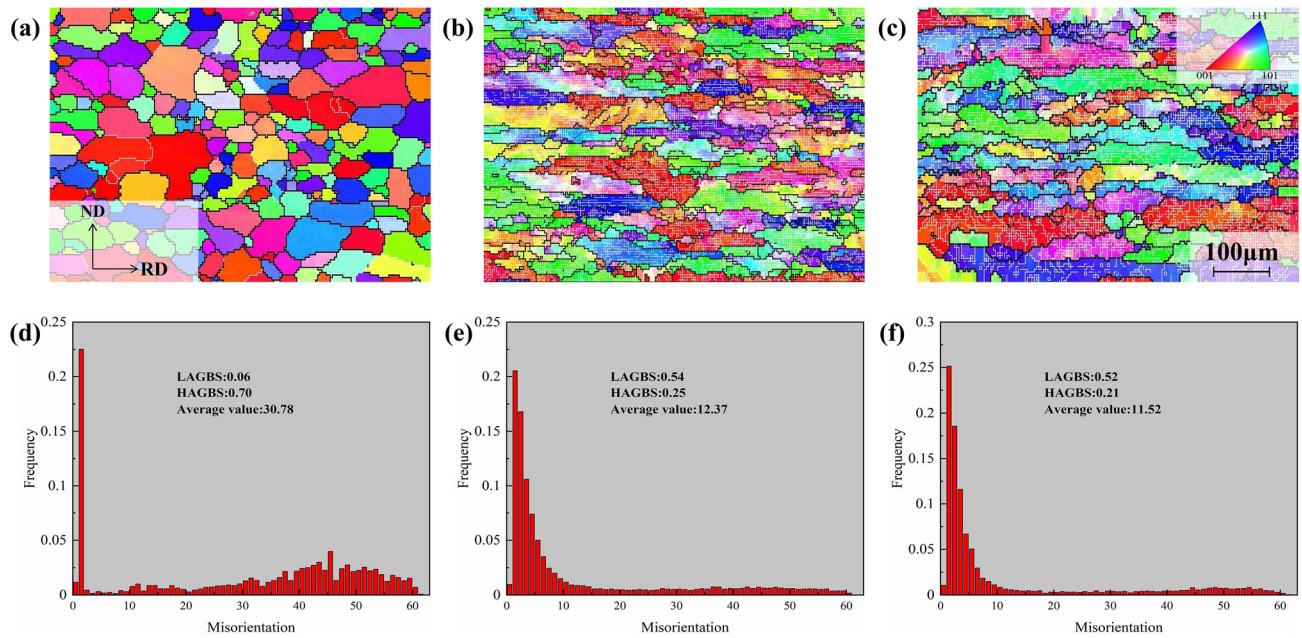

Fig. 9. Distribution of misorientation angle of Al layer (a,d) as-extruded; (b,e) ISR-60%; (c,f) DTAR-60.

degree of DRX. The original structure dominated by subgrains grew up gradually and transformed into recrystallized grains with HAGBs in the DTAR sample.[33]

It is important to note that there was a peak value of around 30° in the Mg layer of as-extruded, ISR-60%, and DTAR-60% plates, which was related to DRX grain boundaries and a lower proportion of LAGBs,[34] indicating the occurrence of pronounced DRX.[35] Moreover, the specimens of as-extruded and DTAR-60% plates have another peak at approximately 86°, which was the typical orientation difference of tensile twins.[36,37]

As shown in Fig. 9, equiaxed grains of the as-extruded aluminum alloy disappeared, and grains extended along the RD direction, presenting a banded structure through two different rolling ways. During the deformation process, the HAGBs

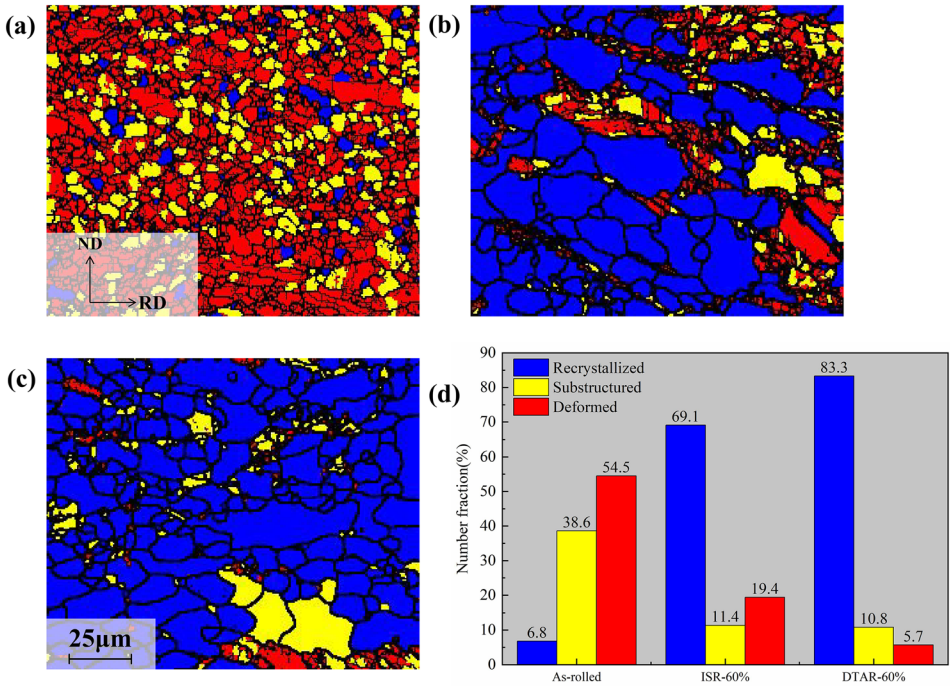

Fig. 10. Recrystallization of Mg layer: (a) as-extruded; (b) ISR-60%; (c) DTAR-60%; (d) Recrystallization statistics chart.

of the recrystallized grain were destroyed, resulting in many LAGBs in the clad plates. The average value of misorientation angle in Al alloy decreased from 30.78° to 12.37°and 11.52°, respectively. The fractions of LAGBs and HAGBs of ISR-60% sample were 0.54 and 0.25, which were a little higher than in the DTAR-60% sample. The reason for the slight difference in misorientation angle in the Al layer is that the speed ratio of asymmetrical rolling is small, which cannot activate the shear strain, so the increase in yield strength is not evident compared with symmetrical rolling.[38] The difference in speed between the two sides of the Al layer in DTAR process was tiny, so the zone shear deformation in asymmetrical rolling could cause some damage to grain boundaries, but the effect on grain deformation was similar to the ISR process.

Recrystallization

Figure 10 illustrates the distribution of recrystallized grains, substructured grains, and large deformed grains of Mg layers in as-extruded, ISR-60%, and DTAR-60%. As seen in Fig. 10d, the fraction of these recrystallized grains was only 6.8%. The number of recrystallized Mg grains increased largely after both rolling processes, so it could be considered that the increase in the fraction of recrystallized grains in the Mg layer occurred in the DRX process. The enormous deformation promoted the breakage and recrystallization of grains. At the same time, due to the low stacking fault energy of Mg alloy, DRX is easy to activate.[39] However, it is worth noting that the number of recrystallized Mg grains in DTAR-60% sample was higher than in ISR-60% sample. The actual deformation caused by one pass of DTAR is higher than that of ISR because of the speed ratio with the same rolling reduction. Therefore, the increase in deformation and accumulative strain was conducive to accelerating the DRX in these grains.

The distribution of recrystallized grains, substructured grains, and large deformed grains of Al layers is shown in Fig. 11. The fraction of recrystallized grains in the as-extruded plate accounted for 71.1%. In the subsequent rolling process, the original structure was destroyed, and many deformation twins were formed, accounting for 96.2% and 96.6%, respectively. The reason for this phenomenon is that the holding time was short, and the deformation of the rolling process did not provide enough driving force for recrystallization. The higher fractions of LAGBs and the high-density dislocation produced during both rolling processes were sufficiently prepared to activate the static recrystallization for subsequent annealing of the composite plate. The grain proportions of ISR-60% and DTAR-60% were similar. Thus, it is reasonable to infer that the mechanical property of composite plates is more dependent on the properties of the Mg base plate by the rolling process.

CONCLUSION

1. The yield strength and ultimate tensile strength of laminates increased with the enhancement of compression, and the yield strength increased

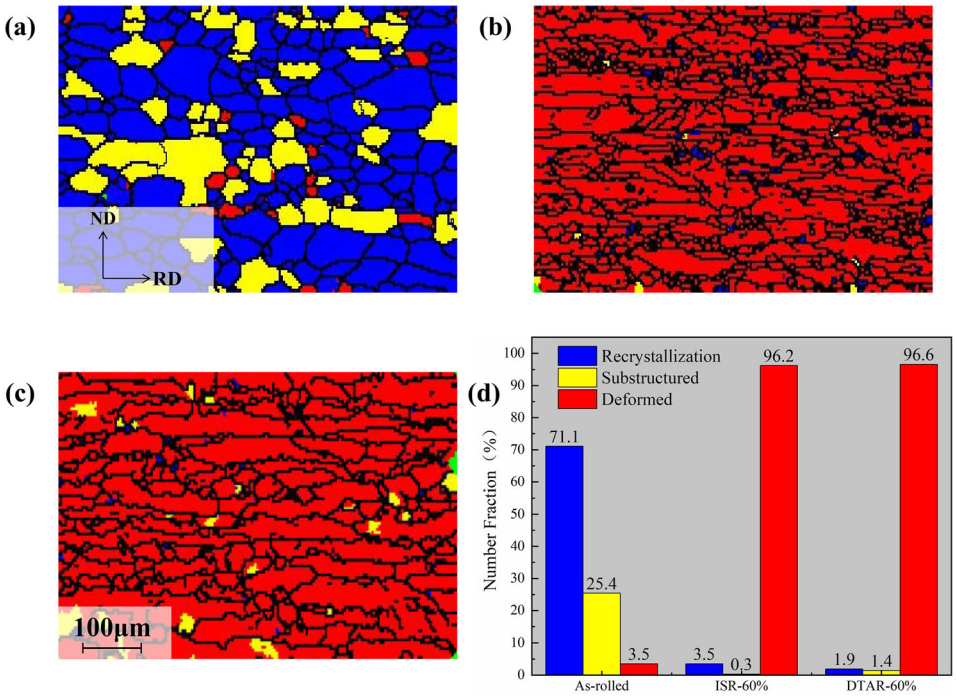

Fig. 11. Recrystallization of Al layer: (a) as-extruded; (b) ISR-60%; (c) DTAR-60%; (d) recrystallization statistics chart.

slightly more than the tensile strength. Compared with the ISR sample, the strength of laminates obtained by DTAR was 205 MPa, which was significantly increased by 10%. At the same time, due to the cross shear deformation zone under DTAR, the hardness of DTAR sample was higher than in ISR sample.

2. The interfaces of Mg/Al laminates were well bonded under different processes, and no intermediate compounds were formed. DTAR provided a strong shear force to form metal bonding in the composite interface. Under different reduction rates, the bonding strength increased in the range of 25%-88%, up to 50 MPa, and the interface morphology of Mg/Al composite plates gradually tended to be flat.
3. The dominant grain on the Mg layer was recrystallized, while the deformation grain was the primary grain on the Al layer when the reduction rate was 60%. The high strain generated in the DTAR converted strain energy into heat energy, which activated the recrystallization and improved the fraction of HAGBs. The fraction of recrystallized grains was up to about 80% under DTAR.

ACKNOWLEDGMENTS

This work was supported by the National Natural Science Foundation of China (U1910213), Taiyuan University of Science and Technology Scientific Research Initial Funding (Grant nos. 20202039 and 20212052)

CONFLICT OF INTEREST

The authors declare that they have no known competing financial interests or personal relationships that could have appeared to influence the work reported in this paper.

REFERENCES

1. K. Kondoh, J. Umeda, H. Sannomiya, T. Luangvaranunt, and H. Nishikawa, *Mater Charact.* 157, 109879 (2019).
2. Z. Chen, D. Wang, X. Cao, W. Yang, and W. Wang, *Mater. Sci. Eng. A* 723, 97 (2018).
3. H. Zuo, Z. Yang, X. Chen, Y. Xie, and H. Miao, *Compos Struct.* 131, 248 (2015).
4. S. Chen, Z. Zhai, J. Huang, X. Zhao, and J. Xiong, *Int. J. Adv. Manuf. Tech.* 82, 631 (2016).
5. Q. Wang, B. Jiang, A. Tang, C. He, D. Zhang, J. Song, T. Yang, G. Huang, and F. Pan, *Mater. Sci. Eng.* 746, 259 (2019).
6. M. Yi, S. Fukushima, S. Sugiyama, and J. Yanagimoto, *Mater. Sci. Eng. A* 624, 148 (2015).
7. Y. Song, E.H. Han, K. Dong, D. Shan, D.Y. Chang, and B.S. You, *Corros. sci.* 72, 133 (2013).
8. J. Tang, L. Chen, G. Zhao, C. Zhang, and J. Yu, *J. Alloy Compd.* 784, 727 (2019).
9. T.T. Zhang, W.X. Wang, J. Zhou, X.Q. Cao, Z.F. Yan, Y. Wei, and W. Zhang, *JOM.* 70, 504 (2018).
10. W. Yang, F. Bo, Y. Xin, H. Rui, H. Yu, and Q. Liu, *Mater. Sci. Eng.* 640, 454 (2015).
11. X.L. Cui, P. Lin, Y.Y. Ma, C.K. Yan, and G. Liu, *JOM.* 71, 1696 (2018).
12. S.K. Lee, S.Y. Lee, and N.Y. Kwon, *Mater. Sci. Eng. A* 628, 1 (2014).
13. J.S. Kim, K.S. Lee, N.K. Yong, B.J. Lee, Y.W. Chang, and S. Lee, *Mater. Sci. Eng. A* 628, 1 (2015).
14. W. Jia, Y. Tang, Q. Le, and J. Cui, *J. Alloys Compd.* 695, 1838 (2017).
15. K.J. Tam, M.W. Vaughan, L. Shen, M. Knezevic, and G. Proust, *Int J Mech sci.* 182, 105727 (2020).

16. C. Tan, S. Xv, L. Wang, Z. Chen, F. Wang, and H. Cai, *Trans. Nonferrous Met. Soc. China.* 17, 41 (2007).
17. Z.Z. Shi, J.Y. Xu, J. Yu, and X.F. Liu, *Mater. Sci. Eng.* 712, 65 (2018).
18. Y. Chai, B. Jiang, J. Song, B. Liu, G. Huang, D. Zhang, and F. Pan, *Mater. Sci. Eng. A.* 746, 82 (2019).
19. G. Nayyeri, R. Mahmudi, and F. Salehi, *Mater. Sci. Eng. A.* 527, 5353 (2010).
20. Q. Wang, Y. Shen, B. Jiang, A. Tang, J. Song, Z. Jiang, T. Yang, G. Huang, and F. Pan, *Mater. Sci. Eng. A* 731, 184 (2018).
21. D. Chang, P. Wang, and Y. Zhao, *J. Alloys Compd.* 746, 259 (2019).
22. D. Chang, X. Dong, and P. Wang, *Rare Met. Mater. Eng.* 49, 85 (2020).
23. X. Li, G. Zu, and P. Wang, *Mater. Sci. Eng. A* 562, 92 (2013).
24. W. Xia, J. Cai, and Z. Chen, *Chin. J. Nonferrous Met.* 20, 1247 (2010).
25. R. Ding, B. Wang, and C. Ren, *Chin. J. Rare Met.* 34, 34 (2010).
26. H. Xiao, Z. Qi, C. Yu, and C. Xu, *J. Mater. Process. Technol.* 249, 285 (2017).
27. H. Nie, W. Liang, L. Zheng, X. Ren, and H. Fan, *J. Mater. Eng. Perform.* 25, 4695 (2016).
28. J. Zhang, L. Wei, Y. Liu, X. Zhao, X. Li, and B. Zhou, *Mater. Sci. Eng. A* 590, 314 (2014).
29. L. Zhang, Q. Wang, W. Liao, W. Guo, B. Ye, W. Li, H. Jiang, and W. Ding, *Mater Charact.* 126, 17 (2017).
30. S.H.S. Ebrahimi, K. Dehghani, J. Aghazadeh, M.B. Ghasemian, and S. Zangeneh, *Mater. Sci. Eng.* 718, 311 (2018).
31. G. Nussbaum, P. Sainfort, G. Regazzoni, and H. Gjestland, *Scr. Metall.* 23(7), 1079 (1989).
32. H. Nie, L. Wei, H. Chen, L. Zheng, C. Chi, and X. Li, *Mater. Sci. Eng. A.* 732, 6 (2018).
33. C. Zhi, L. Ma, Q. Huang, Z. Huang, and J. Lin, *J. Mater. Process. Tech.* 255, 333 (2017).
34. Z. Hua, W. Cheng, J. Fan, B. Xu, and H. Dong, *Mater. Sci. Eng. A* 637, 243 (2015).
35. H. Nie, W. Liang, H. Chen, F. Wang, T. Li, C. Chi, and X.R. Li, *Mater. Sci. Eng. A* 732, 6 (2018).
36. T. Han, G. Huang, Q. Deng, G. Wang, B. Jiang, A. Tang, Y. Zhu, and F. Pan, *J. Alloys Compd.* 745, 599 (2018).
37. M.G. Jiang, C. Xu, H. Yan, G.H. Fan, T. Nakata, C.S. Lao, R.S. Chen, S. Kamado, E.H. Han, and B.H. Lu, *Acta Mater.* 157, 53 (2018).
38. M.Y. Amegadzie, and D.P. Bishop, *Mater. Today Commun.* 25, 101283 (2020).
39. T. Wang, S. Li, H. Niu, C. Luo, and M.U. Bashir, *J. Mater. Res. Technol.* 9, 5840 (2020).